

Das, Bar et al.

Supplemental Data

Table of Contents

Supplementary Text

Supplementary Table 1-2

Supplementary Figures 1-10

Methods:

Isolation of peripheral blood mononuclear cells

Peripheral blood mononuclear cells (PBMCs) were obtained using density gradient centrifugation using Ficoll Paque™ Plus (GE Health Care Life Sciences, UK) as described previously¹ and stored in liquid nitrogen. Plasma was obtained and stored at -80°C.

Flow cytometry to characterize B cell subsets:

Pre- therapy and post- therapy cryopreserved patient PBMCs (anti-PD1; n=8, anti-CTLA-4; n=8 and anti-PD1 and anti-CTLA4 or comb therapy; n=23) were thawed and stained for various B cell markers together using the same antibody cocktail. The following antibodies were used to characterize B cells circulating in the blood. CD19 (SJ25C1) and CD27 (M-T271) (Biolegend, USA), CD38 (HIT2), IgM (G20-127) and CD21 (B-ly4) (from BD Biosciences, USA) were used for identifying naïve (CD19+CD27-), memory (non-switched: CD19+CD27+IgM+, switched: CD19+CD27+IgM-), plasmablasts (CD19+CD27+CD38^{hi}) and CD21^{lo} subset (CD19^{hi}CD21^{lo}). Antibodies against anti-human CD95 (DX2; BD), CD40 (5C3; Biolegend), CD24 (ML5; Biolegend), CXCR4 (12G5, Biolegend), and PD-1 (eBioJ105, eBioscience, USA) or mIgG1 isotype control (eBiosciences) were used to characterize the CD21^{lo} subset. T cells, NK cells and monocytes as well as proliferating CD4 and CD8 T cells were identified using antibodies against CD56 (NCAM 16.2), CD4 (RPA-T4), CD8 (RPA-T8) and CD14 (MφP9) from BD Biosciences and CD3 (SK7) and Ki67 (Ki-67) from Biolegend Inc, USA. Live cells were identified as negatively stained with Live/Dead® Fixable Dead cell stain from Thermo Fisher Scientific, USA. The samples were acquired on BD LSR2™ and the data was analyzed using FlowJo v9.7.5 software (Tree Star Inc., USA).

Single cell mass cytometry:

PBMCs were thawed and stained using metal conjugated antibodies following the manufacturer's instructions (Fluidigm Sciences) as described previously². Supplementary Table 2 lists the anti-body panel used for characterizing B cells. Cell-ID Cisplatin was used to determine Cell viability. Cells were stained with MaxPar Intercalator-Ir prior to acquisition on CyTOF 2 instrument (DVS; Fluidigm Sciences) as previously described. All data were analyzed and plots were generated using the DVS Cytobank software (Cytobank).

Plasma CXCL13 analysis

Levels of chemokine (C-X-C motif) ligand 13 (CXCL13), also known as B lymphocyte chemoattractant (BLC) or B cell-attracting chemokine 1 (BCA-1) were measured in patient plasma before and after treatment with Human CXCL13/BLC/BCA-1 Quantikine ELISA Kit from R&D Systems (USA) following manufacturers protocol.

Single cell RNA sequencing of circulating B cells:

PBMCs obtained from a patient before and after CCB therapy were thawed and sorted to obtain living CD19+ B cells. To perform single cell RNA sequencing of the resulting B cell suspensions, the Chromium Gel Bead and Library Kit (10X Genomics) and Chromium instrument (10X Genomics) were used following the manufacturer's protocol. Libraries were sequenced using the Illumina HiSeq 2500 platform. Reads were aligned, filtered, de-duplicated, and converted

into a digital count matrix using Cell Ranger 1.2 (10X Genomics). Additional quality control (QC) was performed by visual inspection of QC plots using Seurat³. Outlier cells were identified and filtered based on (1) anomalously high/low mitochondrial gene expression (cells with >10% or <1% mitochondrial content were removed) and (2) potential doublets/multiplets, as identified by comparing the number of expressed genes detected by per cell versus the number of unique molecular identifiers (UMIs) detected per cell (cells with greater than 2,250 expressed genes were removed). In addition, we removed 20 potential myeloid cells, identified by the expression of *CD14* and/or *FCN1*. Following these filtration steps, we confirmed the presence of a single B cell cluster in each sample using (1) non-linear dimensional reduction with t-SNE, and (2) the expression of canonical B cell lineage markers (*CD19*, *MS4A1*, and/or *CD79A*; data not shown). A total of 228 pre-therapy and 219 post-therapy B cell transcriptomes passed QC and were retained for further analysis.

Identification of CD21^{lo} and CD21^{hi} B cells from single cell expression profiles:

A previously published gene expression microarray dataset (Affymetrix) consisting of five CD21^{hi} ('conventional') and five CD21^{lo} ('anergic') human B cell samples was downloaded from the Gene Expression Omnibus (GSE13917)⁴. After MAS5-normalization in R using a custom chip definition file (Brainarray version 21; <http://brainarray.mbni.med.umich.edu/brainarray>), all probes were converted to HUGO gene symbols and expression values were log₂ adjusted. Differentially expressed genes between CD21^{hi} and CD21^{lo} B cells were identified as genes with an absolute signal to noise ratio greater than 1.5, an absolute fold change greater than 8, and a q-value less than 0.2. Significance was determined using a two-sided t-test with unequal variance corrected for multiple hypothesis testing by the Benjamini-Hochberg method. These filters yielded 30 and 32 signature genes for CD21^{hi} and CD21^{lo} B cells, respectively (Supplementary Figure 10).

In order to categorize single B cells into CD21^{hi} and CD21^{lo} subsets, we used the following approach. First, all B cells with at least one expressed gene from the CD21^{hi} signature gene set were assigned to the CD21^{hi} B cell subset. Next, we calculated the fraction *f* of expressed genes from the CD21^{lo} gene signature in each B cell. B cells with a corresponding *f* value higher than the 25th percentile of all *f* values >0 in the entire sample were assigned to the CD21^{lo} phenotype. In the event of a tie, the cell was assigned to CD21^{lo}. Using this approach, 89% (397 of 447) of single B cells were assigned to CD21^{hi} and CD21^{lo} subsets.

High throughput BCR Repertoire Sequencing

DNA (4-7 µg) was extracted from cryopreserved PBMCs using the QIAmp® DNA Mini Kit (Qiagen, UK). For some experiments, CD21^{hi} and CD21^{lo} CD19+ B cells were flow sorted prior to extracting the DNA for BCR analysis. A high-throughput BCR IgH survey sequencing was performed via the ImmunoSEQ platform (Adaptive Biotechnologies, USA). B-cell clonal diversity, Somatic hypermutation, V-gene family usage pattern were determined using immunoSEQ Analyzer software (Adaptive Biotechnologies).

Bootstrap analysis:

Due to the limitation of sample size, we performed bootstrap statistical analysis on our discovery data set (Combo treated patients n=23) to test the robustness of our finding (ie greater risk of > grade 3IRAEs in patients with B cell changes). We generated 100 bootstrap data sets by sampling from the discovery data with replacement. Each of the resulting bootstrap data was different from the discovery data and we tested whether B cell changes were associated with higher risk of toxicity within 6 months follow up in each of the bootstrap data. We replicated the findings in discovery dataset 100 % of times. A histogram of the p values was created based on the 100 bootstrap data sets (Supplementary Figure 6).

References:

1. Das R, Verma R, Sznol M, et al. Combination therapy with anti-CTLA-4 and anti-PD-1 leads to distinct immunologic changes in vivo. *J Immunol.* 2015;194(3):950-959.
2. Boddupalli CS, Bar N, Kadaveru K, et al. Interlesional diversity of T cell receptors in melanoma with immune checkpoints enriched in tissue-resident memory T cells. *JCI Insight.* 2016;1(21):e88955.
3. Satija R, Farrell JA, Gennert D, Schier AF, Regev A. Spatial reconstruction of single-cell gene expression data. *Nat Biotechnol.* 2015;33(5):495-502.
4. Isnardi I, Ng YS, Menard L, et al. Complement receptor 2/CD21- human naive B cells contain mostly autoreactive unresponsive clones. *Blood.* 2010;115(24):5026-5036.

Table 1. Patient Characteristics

	Combination(n=23)	CTLA4 (n=8)	PD1 (n=8)
Age (median)	59	67	68
Gender (Male%)	70%	63%	75%
Mutation status			
(BRAF/NRAS/KRAS)*	59% (n=18)	60%(n=5)	50%(n=6)
IRAE			
Grade 1-2	43%	63%	25%
Grade 3-4	43%	13%	13%
Target organ for IRAE			
Skin	83%	38%	13%
Colon	48%	25%	13%
Liver	43%	0%	25%
Pituitary	17%	0%	0%
Thyroid	13%	0%	13%
Platelets (ITP)	4%	13%	0%
Other**	30%	0%	0%
Number of organs affected			
0	13%	25%	62.5%
1	13%	75%	25%
2	22%	0%	12.5%
≥3	52%	0%	0%

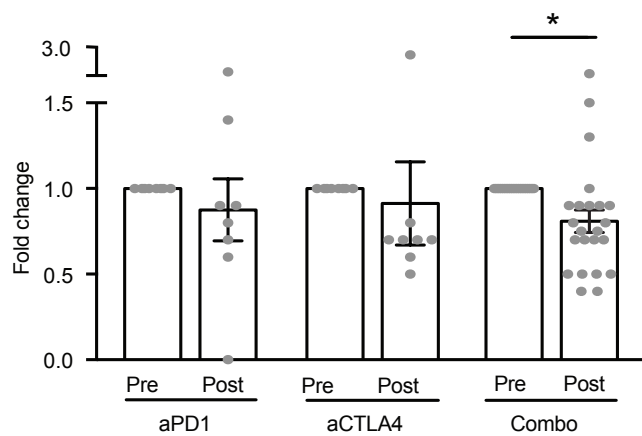
*Percentages calculated from patients with available mutational analysis as specified in parenthesis

**Other: dry eyes, gastritis, arthritis, pancreatitis, nephritis

Supplementary Table 2: CyTOF antibody panel

Antibody	Source	Clone
BCL-6	BD Biosciences	K112-91
CD10	Fluidigm	HI10a
CD117 (c-Kit)	Biolegend	104D2
CD11c	Fluidigm	Bu15
CD138	BD Biosciences	MI15
CD14	Fluidigm	RMO52
CD184 (CXCR4)	Fluidigm	12G5
CD185 (CXCR5)	Fluidigm	RF8B2
CD19	Fluidigm	HIB19
CD20	Fluidigm	2H7
CD21	Fluidigm	BL13
CD22	Biolegend	HIB22
CD23	BD Biosciences	M-L233
CD24	Fluidigm	ML5
CD25	Fluidigm	2A3
CD27	Fluidigm	L128
CD270 (HVEM)	Biolegend	122
CD272 (BTLA)	Fluidigm	MIH26
CD274 (PD-L1)	eBioscience	MIH1
CD276 (B7H3)	Biolegend	MIH42
CD279 (PD-1)	Fluidigm	EH12.2H7
CD3	Fluidigm	UCHT1
CD38	Fluidigm	HIT2
CD40	Fluidigm	5C3
CD44	Fluidigm	IM7
CD45	Fluidigm	HI30
CD5	Fluidigm	UCHT2
CD69	Fluidigm	FN50
CD81	BD Biosciences	JS-81
CD95	Fluidigm	DX2
HLADR	Biolegend	L243
Ig Kappa	Fluidigm	MHK-49
Ig Lambda	Fluidigm	MHL-38
IgD	Fluidigm	IA62
IgM	Fluidigm	MHM88
Ki-67	Fluidigm	Ki-67

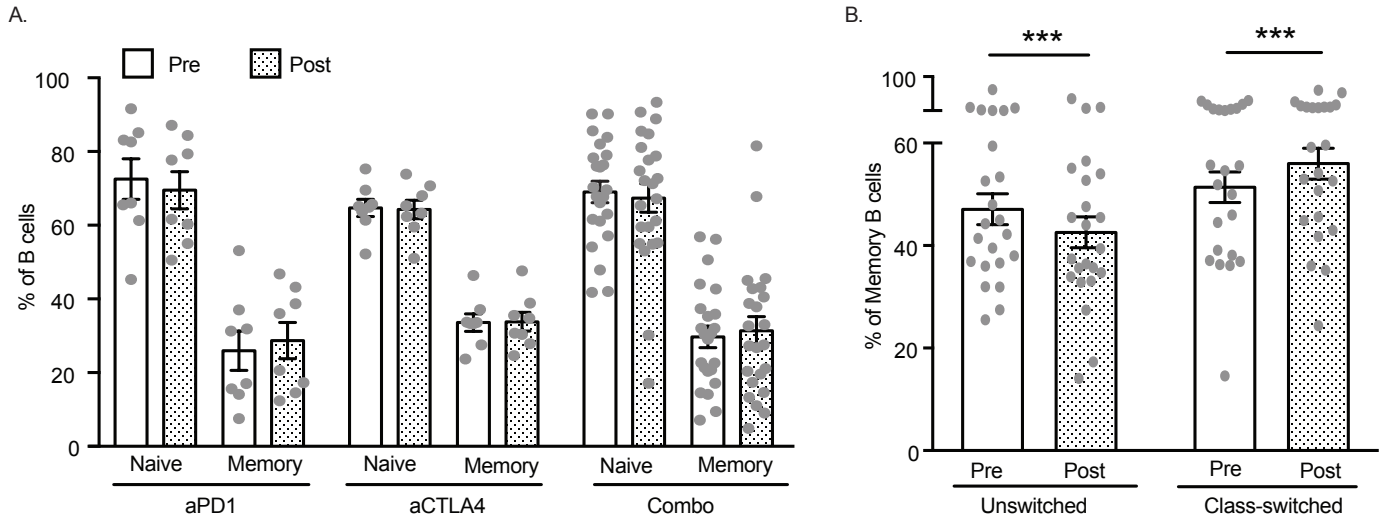
Supplementary Figure 1



Supplementary Figure 1.

Bar graph shows change in absolute numbers of circulating B cells in patients receiving checkpoint blockade therapy with either anti-PD1(n=8), anti-CTLA4(n=8) or combination therapy(n=23). Data shows fold change in B cells compared to pre therapy samples.

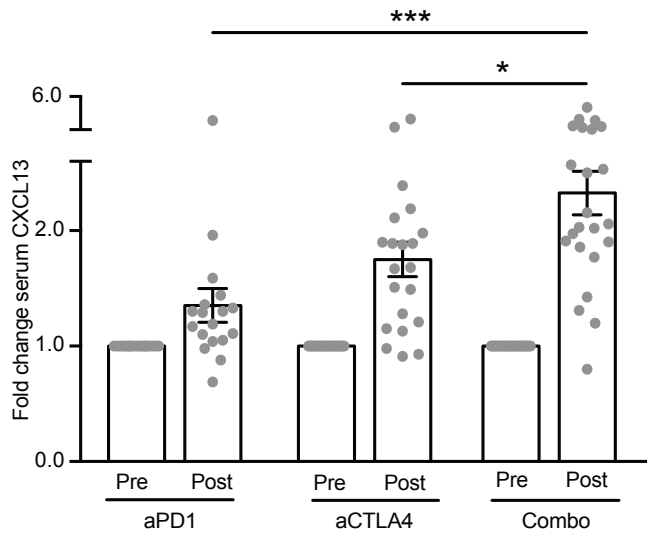
Supplementary Figure 2



Supplementary Figure 2.

PBMCs obtained from patients before (Pre) and after (Post) receiving treatment with either anti-PD1 (α -PD1; n=8) anti-CTLA4 (α -CTLA4; n=8) or concurrent administration of both anti-PD1 and anti-CTLA4 (Combo; n=23) were thawed, stained and analyzed using flow cytometry. A. Circulating naïve (CD19+, CD27-) and memory B cells (CD19+CD27+) before and after checkpoint blockade therapy. B. Unswitched memory (CD19+, CD27+, IgM+) and class-switched memory (CD19+, CD27+ IgM-) B cells in patients before and after receiving combination checkpoint therapy.

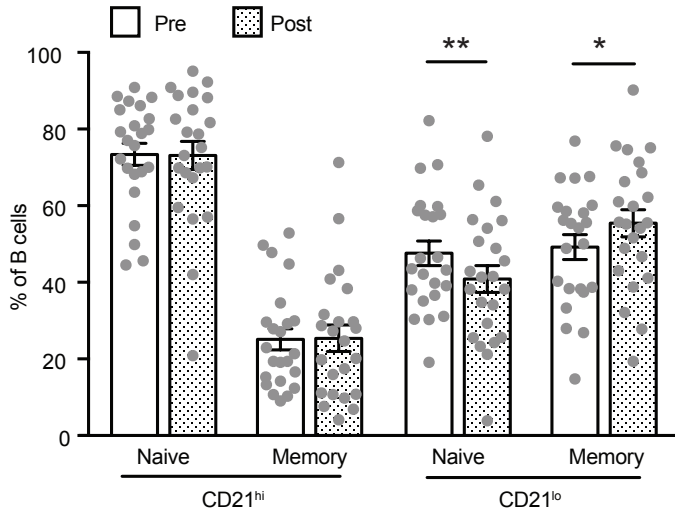
Supplementary Figure 3



Supplementary Figure 3

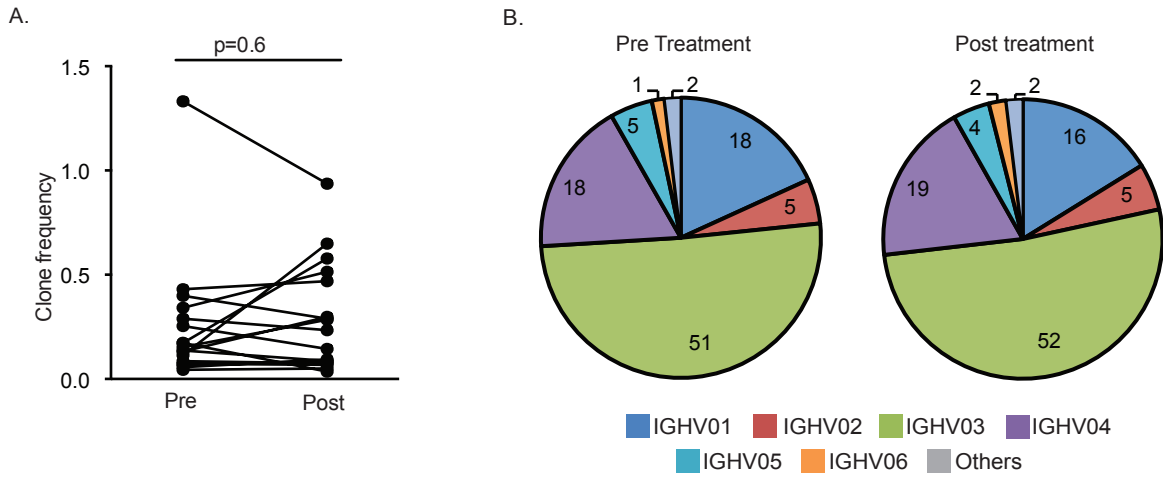
Plasma obtained before and after therapy with ICP blockade was analyzed for changes in CXCL13 using luminex assay. Figure shows changes in plasma CXCL13 levels in patients treated with anti-PD1 (n=18), anti-CTLA4 (n=21) and combination (n=23). This includes all patients (αPD1, αCTLA4 and Combo) used for flow analysis and additional patients treated with monotherapy (αPD1 or αCTLA4) for whom only plasma was available.

Supplementary Figure 4



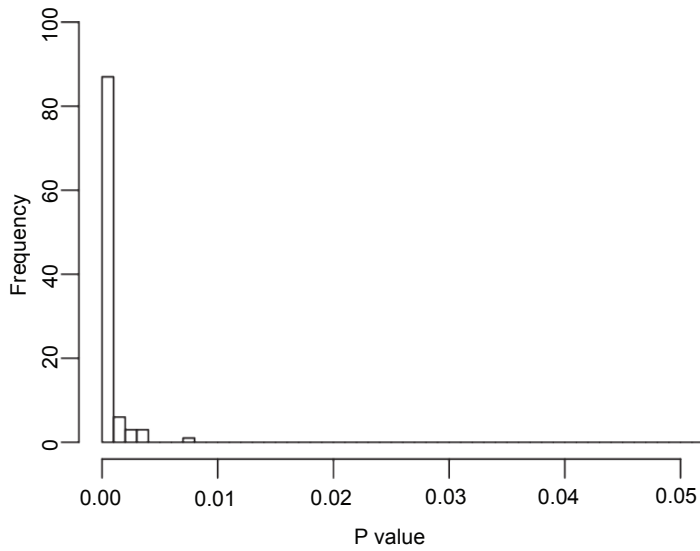
Supplementary Figure 4.
PBMCs obtained from patients before and after receiving combination therapy (n=23) were thawed, stained and analyzed using flow cytometry. Bar graph shows the frequency of naïve and memory CD21^{hi} and CD21^{lo} B cells.

Supplementary Figure 5



Supplementary Figure 5. B cell receptor sequencing was performed on PBMCs obtained from patients before (Pre) and after (Post) one cycle of therapy with ICP blockade (α PD1 n=2; α CTLA4 n=5 and Combo n=10). A. Frequency of the largest B cell clone pre and post therapy in all patients. B. Frequency of the IGHV genes in paired samples before and after CCB therapy in a patient with increased clonality. Numbers represent percent frequency of specific V gene.

Supplementary Figure 6

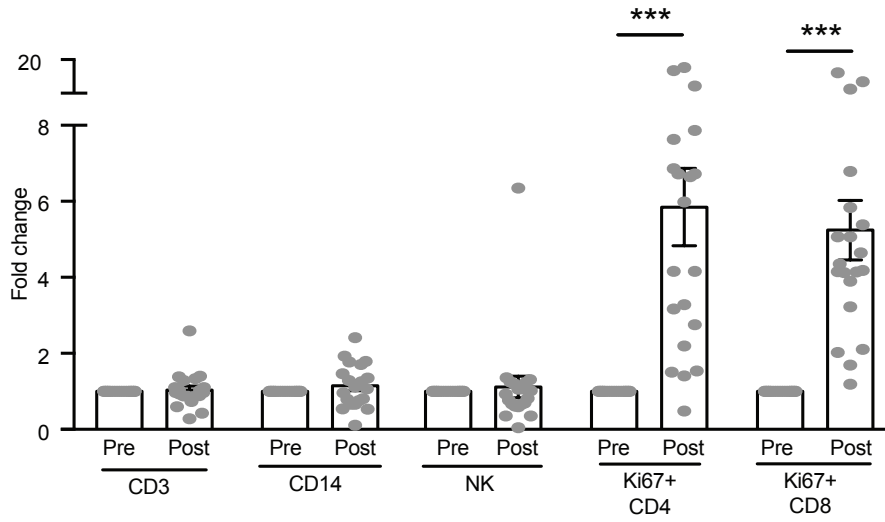


Supplementary Figure 6.

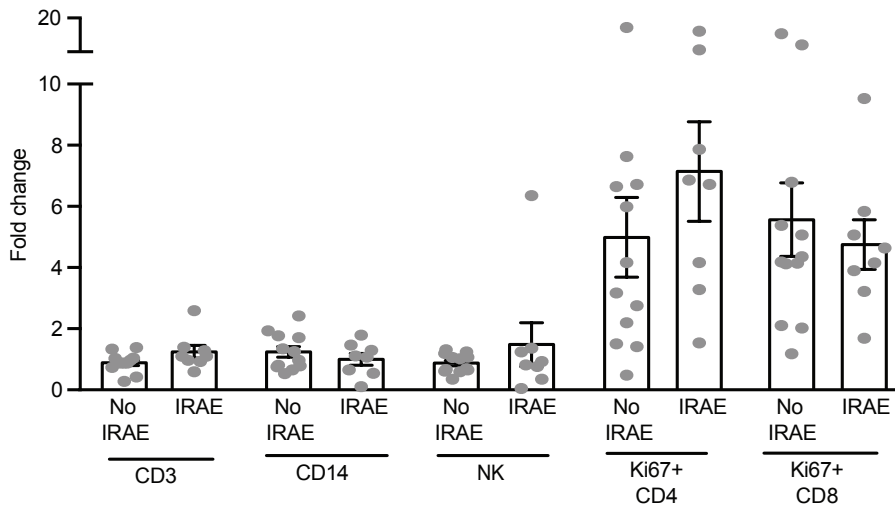
To overcome the limitation of small sample size and test the robustness of the finding that patients with B cell changes following CCB therapy have a greater risk of developing \geq grade 3 IRAE, bootstrap analysis was performed. 100 bootstrap data sets were generated by sampling from the discovery data with replacement. Each of the resulting bootstrap sample ($n=23$) was different from the discovery data and it was tested whether B cell change was associated with higher risk of toxicity within 6 months follow up in each of the bootstrap sample. The findings were reproduced in discovery dataset 100% of times. Figure shows a histogram of the p values created based on the 100 bootstrap samples.

Supplementary Figure 7

A.



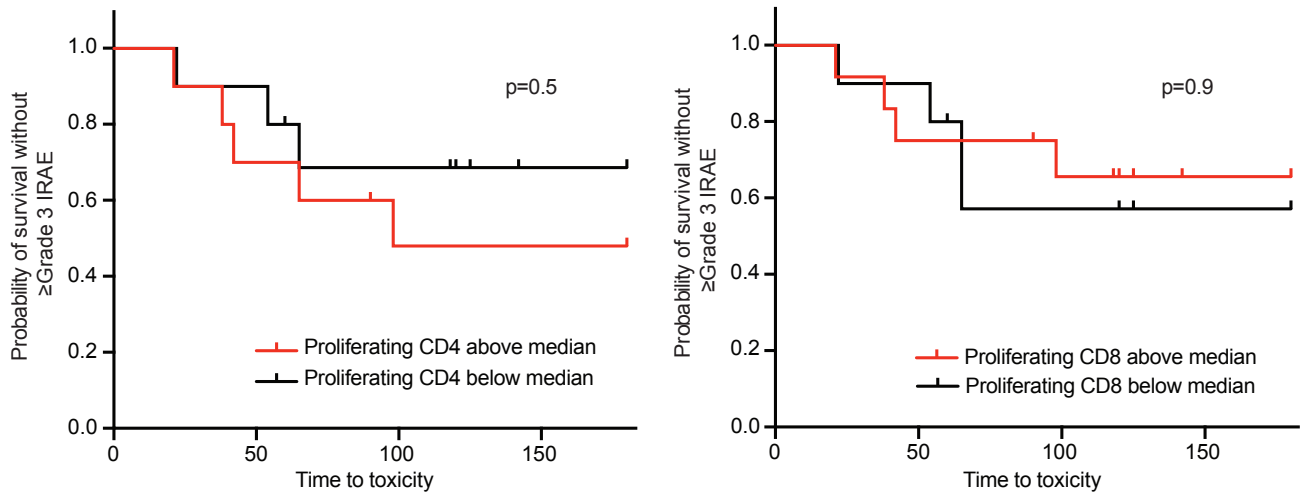
B.



Supplementary Figure 7.

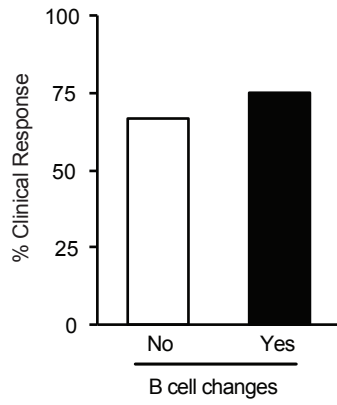
PBMCs obtained from patients before and after receiving CCB therapy (n=20) were thawed, stained and analyzed using flow cytometry. Data show fold change compared to pre-therapy. A. Changes in cellular subsets after therapy. B. Comparison of changes in patients with IRAE (\geq grade 3 IRAE; n=8) or without IRAE (grade 0-2 IRAE; n=12).

Supplementary Figure 8



Supplementary Figure 8. T cell proliferation was analyzed on CD4 and CD8 T cell subsets by Ki-67 staining before and after combination checkpoint therapy (n=20). Patients were divided into two groups based on whether they had increase in CD4/CD8 proliferation above or below the median proliferation for all patients studied. Figure shows toxicity (IRAE \geq grade3) free survival of the two cohorts (p=0.5 and 0.9 respectively for CD4(left) and CD8(right), Log Rank Test).

Supplementary Figure 9



Supplementary Figure 9. Lack of correlation between B cell changes and clinical response. Figure shows percent patients with clinical response (PR+CR) in patients without (n=15) and with B cell changes (n=8). $p>0.9$

Supplementary Figure 10

GeneSymbol	Anergic B cells (CD21 ^{lo})					Conventional B cells (CD21 ^{hi})					GSE13197		
	RA01_	CVID321	CVID214_	CVID218_	RA19_	RA01_con	CVID321_	CVID214_	CVID218_	RA19_con	TTEST Paired	S2N	Fold
	anergic	anergic	anergic	anergic	anergic	ventional	convention	convention	convention	ventional			
	_CD21m	_CD 21m	_CD 21m	_CD 21m	_CD 21m	_CD21p	al_CD21p	al_CD21p	al_CD21p	_CD21p			
FGD4	1.33	2.31	1.73	1.94	2.00	-1.63	-1.33	-1.45	-1.54	-1.79	2.26413E-0	6.39	3.41
DGKG	2.02	2.38	1.46	2.24	3.21	-2.13	-1.99	-2.13	-1.46	-2.81	0.0005613E-	3.92	4.37
LILRB2	3.34	3.94	2.80	1.93	3.66	-3.44	-2.45	-2.34	-3.76	-1.93	3.59287E-0	3.76	5.92
TOX	1.78	1.56	1.54	1.81	1.58	-1.54	-4.39	-2.09	-2.33	-3.71	0.0008688E-	3.39	4.47
ADAP1	1.61	1.14	1.14	1.90	1.71	-1.14	-2.68	-1.87	-2.00	-3.25	0.0006792E-	3.21	3.69
TBX21	2.62	2.17	1.25	1.19	2.55	-1.33	-1.24	-1.19	-1.54	-2.25	0.0012241E-	3.07	3.47
RBPMS2	4.74	2.98	3.28	2.73	4.16	-3.28	-7.16	-3.43	-3.63	-2.73	0.0003735E-	2.92	7.63
ITGAX	2.47	1.96	2.24	1.98	1.33	-1.95	-4.13	-1.33	-2.10	-4.55	0.0006594E-	2.59	4.81
NDRG4	1.01	1.70	1.95	2.51	0.97	-2.20	-0.97	-1.04	-1.30	-1.96	8.55466E-0	2.58	3.12
SIGLEC6	1.87	1.79	1.27	1.22	0.91	-1.49	-0.91	-1.79	-3.20	-3.11	0.0003614E-	2.47	3.51
SDC3	0.85	2.31	1.91	2.57	3.66	-0.94	-1.52	-0.85	-0.96	-1.81	0.0046683E-	2.41	3.48
GTSF1L	2.31	1.85	0.98	1.19	2.87	-1.48	-1.66	-2.30	-2.95	-0.98	1.44151E-0	2.41	3.72
SYT1	1.58	1.17	0.97	1.18	0.77	-0.77	-2.34	-4.18	-2.36	-3.15	0.0011815E-	2.38	3.70
SLC11A1	2.50	1.83	1.82	1.37	3.19	-2.32	-4.88	-2.83	-4.81	-1.37	0.0002640E-	2.38	5.39
TUBB6	0.66	1.37	0.85	1.76	1.59	-1.67	-1.54	-2.84	-0.66	-2.21	0.0005998E-	2.36	3.03
TOX2	2.04	1.35	2.13	2.91	2.26	-1.35	-7.53	-5.37	-2.69	-5.11	0.0022918E-	2.20	6.55
ISL2	2.01	2.70	0.45	2.39	3.77	-1.12	-1.50	-1.32	-0.45	-1.19	0.0036504E-	2.10	3.38
RC3TB2	1.61	2.82	2.21	1.15	1.28	-4.01	-1.63	-2.01	-1.15	-1.43	0.0031209E-	2.10	3.86
SUSD5	1.64	3.00	1.42	2.67	2.84	-5.33	-1.42	-1.53	-2.69	-1.87	0.0017397E-	2.07	4.88
TRERF1	1.86	0.91	1.72	1.81	1.71	-1.71	-2.11	-2.33	-0.91	-5.06	0.0050828E-	2.05	4.02
ATXN1	0.97	0.70	1.42	0.64	1.59	-4.87	-2.80	-0.64	-2.91	-2.52	0.0033392E-	1.98	3.81
LCP2	1.56	0.43	0.81	0.50	1.22	-0.43	-4.32	-2.88	-3.63	-2.43	0.0013642E-	1.86	3.64
SMOC2	1.05	0.94	2.46	0.64	1.56	-0.64	-3.76	-2.28	-5.65	-3.81	0.0041510E-	1.76	4.56
T	3.35	3.59	2.60	0.77	2.23	-0.77	-1.31	-1.24	-1.99	-1.40	0.0012988E-	1.75	3.59
MAGEA11	1.74	1.45	1.87	0.20	1.31	-1.95	-0.20	-1.42	-2.55	-3.31	0.0028678E-	1.75	3.20
RIN2	0.66	2.74	2.80	1.70	1.91	-3.34	-0.88	-0.89	-0.66	-1.66	0.0002586E-	1.74	3.45
LOC100505501	2.62	1.01	2.18	1.77	1.57	-5.43	-6.60	-1.01	-1.02	-4.38	0.0071961E-	1.74	5.52
SOX5	0.98	0.92	1.47	1.83	0.53	-3.51	-2.17	-0.53	-0.66	-3.08	0.0019762E-	1.67	3.13
SLCO4C1	0.96	1.92	1.17	0.75	1.77	-5.41	-2.19	-0.75	-2.47	-1.39	0.0070938E-	1.63	3.76
PHEX	0.86	0.34	1.56	1.32	1.08	-3.36	-1.35	-0.34	-2.00	-4.44	0.0097779E-	1.59	3.33
TBKBP1	0.93	0.95	0.33	1.72	2.67	-3.54	-1.36	-2.21	-0.33	-2.31	0.0057225E-	1.56	3.27
BCL11B	1.84	0.51	0.89	1.05	2.07	-0.80	-1.99	-0.51	-3.88	-1.86	0.0072493E-	1.56	3.08
LOC101929759	-0.81	-1.88	-2.36	-2.83	-0.44	3.16	1.13	0.44	1.12	1.42	0.0013541E-	-1.54	-3.12
CORO2B	-5.17	-0.31	-1.64	-2.30	-2.10	2.99	3.36	0.31	2.93	2.23	0.0103505E-	-1.56	-4.67
CTTNBP2NL	-0.59	-1.51	-0.28	-2.26	-3.04	2.22	0.28	1.78	1.62	2.36	0.0085212E-	-1.62	-3.18
THR3	-0.76	-4.34	-1.37	-5.74	-3.56	0.76	0.80	1.32	1.74	2.45	0.013798E-	-1.64	-4.57
SPINK2	-3.85	-4.82	-3.25	-4.77	-0.20	1.16	0.49	-0.20	0.71	1.21	0.0069009E-	-1.69	-4.08
CCSER1	-4.05	-0.73	-0.62	-1.68	-1.92	1.62	1.18	1.86	1.38	0.62	0.0090405E-	-1.69	-3.13
VPREB3	-0.73	-1.82	-4.13	-2.67	-0.87	2.26	2.62	0.73	1.73	3.18	0.000194E-	-1.78	-4.15
MTCL1	-1.31	-0.40	-2.01	-0.90	-2.52	3.77	3.72	2.41	2.44	0.40	0.000497E-	-1.79	-3.97
MEGF6	-6.34	-5.24	-2.19	-5.81	-0.91	1.14	1.54	1.25	0.91	2.62	0.0030109E-	-1.82	-5.59
LOC105374407	-0.86	-0.97	-1.84	-3.01	-1.02	3.12	1.68	1.25	0.86	1.62	0.0003543E-	-1.84	-3.24
LAMC1	-1.06	-3.39	-0.92	-1.63	-0.73	1.85	0.73	1.95	1.66	2.78	0.0001275E-	-1.84	-3.34
JAKMIP2	-1.03	-0.61	-1.79	-3.58	-2.81	1.35	1.97	1.17	0.61	1.00	0.0008260E-	-1.84	-3.19
SLCO5A1	-1.61	-1.29	-3.74	-2.65	-0.79	1.58	1.80	0.79	2.51	0.89	0.0043643E-	-1.87	-3.53
MYO1B	-1.22	-1.50	-1.59	-2.73	-5.92	1.80	2.27	1.22	2.34	1.96	0.0083702E-	-1.88	-4.51
FAM26F	-0.42	-1.88	-1.70	-2.52	-1.98	2.65	1.65	0.42	1.43	1.14	0.0005009E-	-1.98	-3.16
NIPAL4	-3.59	-4.72	-2.42	-1.06	-1.74	1.06	1.93	1.10	1.26	2.71	0.0037546E-	-1.99	-4.32
RAPGEF5	-2.67	-3.29	-0.66	-3.47	-3.30	0.66	2.89	1.17	3.18	1.42	0.007072E-	-1.99	-4.54
P2RY14	-3.80	-0.49	-3.03	-2.90	-2.67	1.99	2.43	1.78	0.49	1.66	0.0011351E-	-2.16	-4.25
SH2D3A	-3.04	-1.71	-2.06	-1.74	-0.52	0.99	1.15	0.52	1.47	1.81	0.0005207E-	-2.17	-3.00
ZCCHC18	-0.88	-0.92	-1.68	-3.05	-1.68	3.13	2.42	2.12	0.88	2.78	2.70413E-0	-2.24	-3.91
FAM111B	-1.79	-1.99	-1.18	-3.85	-2.74	1.18	4.13	2.87	3.54	2.17	0.0027890E-	-2.33	-5.09
SPRY1	-1.40	-1.24	-0.83	-1.11	-2.27	2.40	0.83	1.55	3.30	2.29	0.0026135E-	-2.33	-3.44
SLC38A11	-1.56	-1.74	-2.29	-3.31	-2.10	1.91	4.60	3.97	1.56	4.81	0.0008637E-	-2.52	-5.57
SERPINB9P1	-2.55	-2.03	-2.05	-3.43	-0.85	1.55	1.88	0.97	0.85	1.41	0.0007679E-	-2.58	-3.51
SCN3A	-3.74	-0.97	-3.00	-2.10	-2.49	2.56	2.21	1.46	1.91	0.97	0.0014854E-	-2.58	-4.28
CR1	-0.94	-2.54	-1.30	-2.63	-1.71	2.01	1.60	1.47	1.24	0.94	0.0004193E-	-2.85	-3.28
STEAP1B	-3.12	-2.15	-1.10	-3.35	-3.14	1.10	2.82	2.41	1.87	1.94	0.0001425E-	-2.89	-4.60
DCBLD2	-0.97	-2.15	-2.23	-2.77	-1.89	1.84	1.57	1.80	1.00	0.97	0.0001708E-	-3.16	-3.44
CR2	-1.60	-4.18	-2.26	-3.53	-2.62	2.89	2.44	1.60	2.16	2.86	0.0004009E-	-3.36	-5.23
ZDHHC19	-1.94	-1.65	-2.90	-2.68	-1.15	1.76	1.72	1.15	2.01	1.73	0.0002566E-	-3.60	-3.74

Supplementary Figure 10.

Analysis of previously published gene array microarray dataset (affymetrix) GSE13197 (Isnardi et al Blood 2010). Heat map shows differentially expressed genes between CD21^{lo} and CD21^{hi} B cell subsets. These genes were used to identify CD21^{lo} and CD21^{hi} B cells in the single cell RNA-Seq analysis as described in the methods section.